

## Speciation and mass distribution of mercury in a solid refuse fuels power plant

Eun-Song Lee, Sang-Yeop Lee, Soo-Jin Cho, Yong-Chil Seo, Seong-Heon Kim<sup>†</sup>, and Ha-Na Jang<sup>†</sup>

Department Environmental Engineering, Yonsei University, 1, Yonseidae-gil, Wonju 26493, Korea

(Received 23 April 2021 • Revised 26 July 2021 • Accepted 27 July 2021)

**Abstract**—The behavior of mercury (Hg) species during thermal cogeneration was analyzed in a 10 MWh solid refuse fuel (SRF) utility boiler using a selective non-catalytic reduction unit, semi-dry reactor, and fabric filter with activated carbon injection for air pollution control from the facility. The annual Hg inflow into this facility is 24.2 (from 9.2 to 33.3) kg. The Hg species in flue-gas at inlet and outlet of the air pollution control devices (APCDs) were observed to be a mixture of 14.4  $\mu\text{g-Hg}/\text{Sm}^3$  of particulate mercury, 2.6  $\mu\text{g-Hg}/\text{Sm}^3$  of oxidized mercury, and 15.6  $\mu\text{g-Hg}/\text{Sm}^3$  of elemental mercury and another mixture of 0.0 of particulate mercury, 0.3 of oxidized mercury, and 11.0 of elemental mercury, respectively. Elemental mercury was the major component in the combustion residue. In the emission assessment, the mass distribution of Hg of fly ash, bottom ash, and stack emission was determined as 67% (16.2 kg/yr), 2.0% (0.47 kg/yr) and 31% (7.5 kg/yr), respectively. Although elemental mercury was captured by APCDs configuration, it is best to chemically capture the air-emission mercury. Evaluation of Hg stability was tested for the fly ash by sequential extraction procedure method.

Keywords: Mercury, Emission, SRF, Speciation, Mass Distribution

### INTRODUCTION

The United Nations Environmental Programme (UNEP) has developed a legally binding treaty on mercury (Hg) for global application [1]. The Minamata Convention on Mercury was adopted in 2013 through several deliberations of the Intergovernmental Negotiating Committee, which aimed to reduce Hg emissions and protect human health and the environment. Hg contained in the combustion flue gas mainly consists of elemental  $\text{Hg}^0$ , oxidized  $\text{Hg}^{2+}$  and particle-bound  $\text{Hg}_p$ . It is known to be difficult to control  $\text{Hg}^0$  unless it is oxidized across air pollution control devices (APCDs) [2]. A previous study reported that  $\text{Hg}^0$  can be controlled by utilizing the co-beneficial effect by APCDs designed to control  $\text{NO}_x$ ,  $\text{SO}_x$ , and particulate matters [3]. However, a re-emission problem in the wet scrubber due to sulfite ions and pH was identified [4]. As such, the behavior of Hg in the process was found to be affected by various parameters and has different emission characteristics depending on the spent fuels and operation conditions. For the integrated management of Hg emission sources, article 8 categorized major sources of anthropogenic emission in annex D as follows: coal-fired power plants (CPPs) and industrial boilers, non-ferrous metal production facilities, waste incinerator and cement clinker production facilities [1]. Among them, CPPs are considered to be the largest anthropogenic source.

Global Mercury Assessment (GMA) reports the amount of Hg emission every five years [5]. As per these reports, Hg air emissions from CPPs decreased from 316 ton-Hg/yr in 2013 to 292 ton-Hg/yr in 2018, whereas those from waste incineration facilities increased from 6.2 ton-Hg/yr to 15.0 ton-Hg/yr in the 2019 year. Further, Hg

emissions from CPPs were simultaneously reduced from 2003 to 2019 due to the improved air pollution control technologies and stricter emission standards of air pollutants such as  $\text{SO}_x$ ,  $\text{NO}_x$ , and particulate matter [6]. The use of the hybrid filter coated with activated carbon in fabric bags increased the Hg removal efficiency from 4.3% to 15.86% compared with typical plants [7]. Cao et al. [8] estimated the Hg oxidation efficiency when halogen-based gases were injected into the boiler and SCR process. Maximum Hg oxidation efficiency by HBr, HI, and HF between 600 to 640 K was reported to be 85%, 79%, and 34%, respectively [8]. Pudasainee et al. [3] compared the control efficiency of Hg for the unit process and the maximum Hg removal efficiency of the overall plants by the co-beneficial effect. It was reported that APCDs showed a Hg control efficiency of up to 80% via a simple arrangement of the SCR-ESP-FGD orders [3]. As such, it can be said that Hg emissions have been reduced through continuous efforts. However, the top 20 CPPs emitting the most amount of air pollutant at the global level are concentrated in East Asia, including China [9]. At times, early retirement of CPPs located in densely populated areas has been required. In addition, the average ages of CPPs in the U.S. and EU are between approximately 30 to 50 years. Various technologies have been developed to replace coal-based power production with eco-friendly energy sources such as hydrogen, solar, and wind power. Ahmad et al. [10] investigated the behavior of heavy metals including Hg through sequential APCDs. It was found that majority of mercury was removed in the fabric filter and in a major form of oxidized  $\text{Hg}^{2+}$  [10].

Solid refuse fuel (SRF) utility boiler for thermal cogeneration was derived to address various environmental issues such as increasing waste, saving fossil fuels, and developing renewable energy. SRF was sub-categorized into refuse-derived fuel (RDF) and refuse plastic fuel (RPF). The process starts with combustible materials and then proceeds through a series of mechanical screening from MSW. The

<sup>†</sup>To whom correspondence should be addressed.

E-mail: seongheo@yonsei.ac.kr, janghn74@hanmail.net

Copyright by The Korean Institute of Chemical Engineers.

Korean SRF product standards such as those for moisture, ash, chlorine, sulfur, and Hg are strictly applied [11]. However, Hg contained in packages and paints from discharged waste is likely to be concentrated in the SRF during the screening process.

Although SRF thermal utility is similar to the APCDs arrangement of conventional waste incineration facilities [2,12,13], SRF has a relatively high chlorine concentration compared to MSW. The existence of chlorine can affect the behavior of gaseous Hg during the combustion process. Chlorine can also get converted into the hydrogen chloride gas in the  $\text{Hg}^0$  oxidation process and directly converted to  $\text{HgCl}_2$  with a higher oxidation rate [14,15]. Meanwhile,  $\text{Hg}^{2+}$  can be easily controlled with the help of wet flue gas desulfurization devices (WFGDs). According to the process optimization guidance (POG) for the Hg emission control program developed by UNEP, the heating value of fuels is the major factor affecting the oxidation of Hg in flue gas [16]. A relatively higher heating value of SRF would generate different species variation properties in flue gas.

Ahmad et al. [17] reported the behavior of Hg in a municipal solid waste incinerator without including  $\text{Hg}_p$  [17]. The concentration of  $\text{Hg}_p$  is directly related to the Hg content of fly ash and waste, and the potential for getting released into leachate would cause a secondary pollution problem. Yi and Jang [18] reported SRF life cycle assessment and energy recovery from SRF utilized for energy generation plants [18].

However, studies on Hg stability assessment for emissions and incineration residues are still lacking. Although the number of driving cases of SRF utility plants is increasing worldwide, there is still a lack of research on measuring and evaluating the stability of Hg in each environmental media.

In this study, the distribution characteristics and speciation of Hg ( $\text{Hg}_p$ ,  $\text{Hg}^{2+}$ , and  $\text{Hg}^0$ ) in an SRF utility plant for thermal cogeneration were analyzed. In addition, the stability of Hg was assessed by applying a sequential extraction procedure to derive the best environmental practices for the integrated management of Hg emission into environment and to contribute to the estimation of the national Hg air emission data.

## MATERIALS AND METHODS

### 1. Configuration of the APCDs

The facility utilized in this study was a circulating fluidized bed type of an SRF utility boiler for thermal cogeneration. The daily consumption of refuse-derived fuel and plastic fuel was approximately 80 tons and the generating capacity was 10 MWh. The facility consisted of one selective non-catalytic reduction (SNCR), one semi-dry reactor (SDR) and a few fabric filters as APCDs in series, which were originally designed and developed to enhance the control of  $\text{SO}_x$  and filterable particulate matters. SNCR was attached to reduce the fuel  $\text{NO}_x$ , thermal  $\text{NO}_x$ . Urea and ammonia were injected into the nozzle as reductants. A specific operation temperature is required to initiate the reaction, otherwise ammonia will pass through SNCR unreacted. Additionally, the lime/limestone slurry was injected into the SDR to remove the  $\text{SO}_2$  in the flue gas [4]. Activated carbons are injected in the FF process step to adsorb the heavy metals in the flue gas; finally, the clean flue gas was released to the atmosphere. This type of an SRF utility boiler and APCDs configuration

is similar to that of the typical municipal solid refuse incinerator [19]. Another type of the SCR system targeting  $\text{NO}_x$  was not included in this utility.

### 2. Sampling and Hg Analysis

Samples from each process were collected to estimate the overall Hg flow and mass distribution, including the injected substances or fuel such as fluidizing materials, urea, and lime/limestone.

Hg sampling was triplicated at both the upstream and downstream of the APCD system. The standard test method was applied to analyze the Hg emission concentration and speciation in flue gas for particle-bound ( $\text{Hg}_p$ ), oxidized ( $\text{Hg}^{2+}$ ), and elemental ( $\text{Hg}^0$ ) [20]. Isokinetic sampling was performed to collect particulate matters and sufficient gas volume in the flue gas stream. To prevent the internal surface adsorption of the particulate matter collected for sampling, the probe was equipped with a nozzle, connecting tube, and liner made of quartz. Among the Hg species,  $\text{Hg}_p$  in particle phase was collected in an 88R filter (Advantec, thimble filter) in front of the probe, and the difference in filter weight before and after sampling was recorded. Gaseous Hg was sampled by an impinger train filled with ice. The  $\text{Hg}^{2+}$  was absorbed into three consequent impingers filled with 1 N potassium chloride solution, whereas  $\text{Hg}^0$  was absorbed in an impinger filled with 5% nitric acid and 10% hydrogen peroxide solution and three additional impingers filled with 4% permanganate solution. The last impinger was filled with silica gel for moisture removal. The recovery of the solution was performed immediately after sampling.

The US EPA methods 7471a and 7470a were used for the pre-treatment of solid and liquid phase samples, respectively [21,22]. For the pre-treatment, 0.2 g of solid and 100 ml of liquid samples were added in a borosilicate brown bottle. Aqua regia and sulfuric acid were added to dissolve each sample. For Hg oxidation and reduction, 15 ml of a 5% (W/V)  $\text{KMnO}_4$  solution and 6 ml of 12% (W/V)  $\text{SnCl}_2$  were used. Hg content was analyzed by cold vapor atomic absorption spectroscopy (RA915+ ZEEMAN, Lumex Ltd).

### 3. Manufacturing Processes and the Characteristics of Solid Refused Fuel

The composition of the fuels significantly affects the emission characteristics of air pollutants during combustion. The manufacturing process of SRF typically consists of several mechanical steps such as screening, drying, mixing, and casting. First, sand and inorganics are separated from municipal solid wastes by one sloping unit and two magnetism separators in series. And then, moisture is removed by high temperature dry-air. The temperature of the inlet and outlet of the dry kiln is about 590 °C and 160 °C, respectively. The pre-treated materials are pulverized to the size of less than 25 mm using a V-ROTOR type shredder.

The characteristics of SRF were analyzed to assure the quality as fuel and to inspect any potential generation of pollutants. Elemental analysis (EA1110, Thermo Finnigan Co.) was conducted for the analysis of C, H, O, N and S contents. The proximate analysis was conducted using a thermogravimetric analyzer (TGA701, LECO Co.). In addition, the concentration of chlorine in the sample was analyzed by ion chromatography (ICS-2100, Dionex Co.). The results of the basic properties of SRF are shown in Table 1.

### 4. Sequential Extraction Procedure for Hg

The sequential extraction procedure (SEP) was applied to eval-

**Table 1. Basic characteristics analysis results of SRF**

Analysis	RDF	RPF	Unit
Proximate analysis	Moisture	4.2	3.7
	Volatile	78.3	84.3
	Ash	13.4	9.3
	Fixed carbon	4.1	2.7
Elemental analysis	C	54.2	65.4
	H	6.7	10.5
	N	0.5	0.7
	O	23.5	12.4
	S	<0.05*	<0.05*
Ion chromatography	Cl	0.6	0.8
Low heating value		5,710	6,440

\* Below detection limit of analysis

uate the Hg stability of emitted residues from each APCDs unit [23]. The SEP consists of five steps with solvents at different pH levels (Table 2). Depending on the pH of the solvent and solubility of various kinds of Hg compounds, different dominant Hg compounds were leached out at each step. In all steps, 0.4 g of solid sample and 40 ml of solvent were used. Each sample with solvents was shaken for 18±4 h at 40 rpm by a rotary stirring device except for step F5. After washing twice with deionized water, centrifugation was performed for 20 min at 1,600 g of relative centrifugal force (RCF) using 1580R to exchange the solvent. Solvents sample at each step were pretreated in accordance with EPA method 7470a. The recovery rate was determined by the ratio of Hg content in SEP solvent to that of the raw sample.

Recovery rate (R. R)

$$= \frac{\text{Total Hg content in SEP solvent (mg-Hg)}}{\text{Hg content of raw sample (mg-Hg)}} \times 100 \quad (1)$$

## RESULTS AND DISCUSSION

### 1. Estimation of Hg Inflow and Analysis of the Basic Characteristics of the Fuel

Hg concentrations of the input material are presented in Table 3. RDF and RPF were supplied at a constant rate of 80 tons/day for onsite testing. In addition, limestone/lime, urea, and fluidizing sand were used for the operation of the SRF power plant. Based on 365 days of annual operation, the amount of inflow Hg in the SRF power plant was estimated to be an average of 24.2 (9.2 to 33.3) kg. Among these, inflow Hg into RDF and RPF accounted for approximately 54.1% and 37.6%, respectively. Unlike conventional SRF power plants, kaolin was mixed with fluidized sand to improve the control efficiency of gaseous pollutants such as NO<sub>x</sub> and SO<sub>x</sub> [24]. Kaolin has also been reported to be effective in controlling not only HCl but also particulate matters in flue gas [25]. For this reason, Kaolin indirectly contributed to the reduction of Hg<sup>2+</sup> and Hg<sub>0</sub>. The Hg content in Kaolin was 0.62 (0.41 to 0.74) mg-Hg/kg and accounted for approximately 3.7% of the total Hg inflow.

The management of input fuel is required to be given a high priority and is considered to be the best practice for reducing environmental emissions of Hg. The key combustion factors of SRF that might affect the composition of flue gas and species of Hg in the process are detailed in Table 1. The moisture content of SRF was less than 5% without any sulfur content, making it adequate as a fuel. However, compared with RDE, RPF had 0.2% higher chlorine content, and the higher low heating value by 730 kcal/kg. In

**Table 2. Method of sequential extraction procedure [23]**

Step	Extraction solvent	Extraction process	Fraction definition	Typical Hg compound
F1	0.5 M NH <sub>4</sub> Cl	At each step,	Ion-exchangeable Hg	HgCl <sub>2</sub> , HgSO <sub>4</sub>
F2	0.1 M CH <sub>3</sub> COOH +0.1 M HCl	centrifuging for 18±4 h (30 rpm at room temp.)	Acid-soluble Hg	HgO, HgSO <sub>4</sub>
F3	M KOH	& centrifuged 1,600 g	Organic matter-bound Hg	Hg-humics, HgCl
F4	12 M HNO <sub>3</sub>	(RCF) for 20 min	Metallic bound Hg, Elemental Hg	Hg <sup>0</sup> , (Hg amalgam)
F5	Aqua regia	Static 12 h (at room temp.)	Sulfide & residual Hg	HgS, residual Hg

**Table 3. Hg concentration of input materials into SRF power plant**

Materials	Input amount (ton/day)	Hg concentration (mg-Hg/kg)			Hg inflow per year (kg-Hg/yr)	Fractions (%)
		Avg.	Max.	Min.		
RDF	80	0.45	0.64	0.12	13.1 (3.5-18.7)	54.1
RPF	80	0.31	0.42	0.14	9.1 (4.1-12.3)	37.6
Fluidizing sand	4.9	0.16	0.24	0.10	0.3 (0.2-0.4)	1.2
Limestone	14.5	0.06	0.06	0.06	0.3	1.2
Slaked lime	0.4	0.20	0.25	0.15	0.0	0.2
Kaolin	4	0.62	0.74	0.41	0.9 (0.6-1.1)	3.7
Urea	0.9	1.43	1.44	1.41	0.5	2.0
Total					24.2 (9.2-33.3)	100

addition, the RDF showed a larger variation of Hg content of approximately 0.52 mg-Hg/kg, which would consequently increase the uncertainty of the Hg emission.

**2. Hg Speciation in Flue Gas and Mass Distribution for SRF Power Plant**

The APCDs configuration and operating conditions are important parameters for the removal of gaseous Hg in the plants. In general, Hg<sup>2+</sup> is easily controlled by a wet type of ADCDs such as SDR and FGD. A major portion of Hg attached to particulate matter is

removed by filtration and adsorption across ESP, FF, ACI, and cyclone. Whereas the removal efficiency of Hg<sup>0</sup> by direct adsorption is not so high. Hg speciation results of both upstream and downstream flue gases of APCDs are shown in Fig. 1 and Table 4. In the previous study about Hg species in the circulation fluidized bed type of MSWI [19], Hg<sup>2+</sup>, Hg<sup>0</sup>, and Hg<sub>p</sub> accounted for 95.5%, 4.1%, and 0.4%, respectively. The total Hg concentration in flue gas is approximately 10 to 60 µg-Hg/Sm<sup>3</sup>. Although APCDs and boiler types of MSWI are similar to those of the present facility,

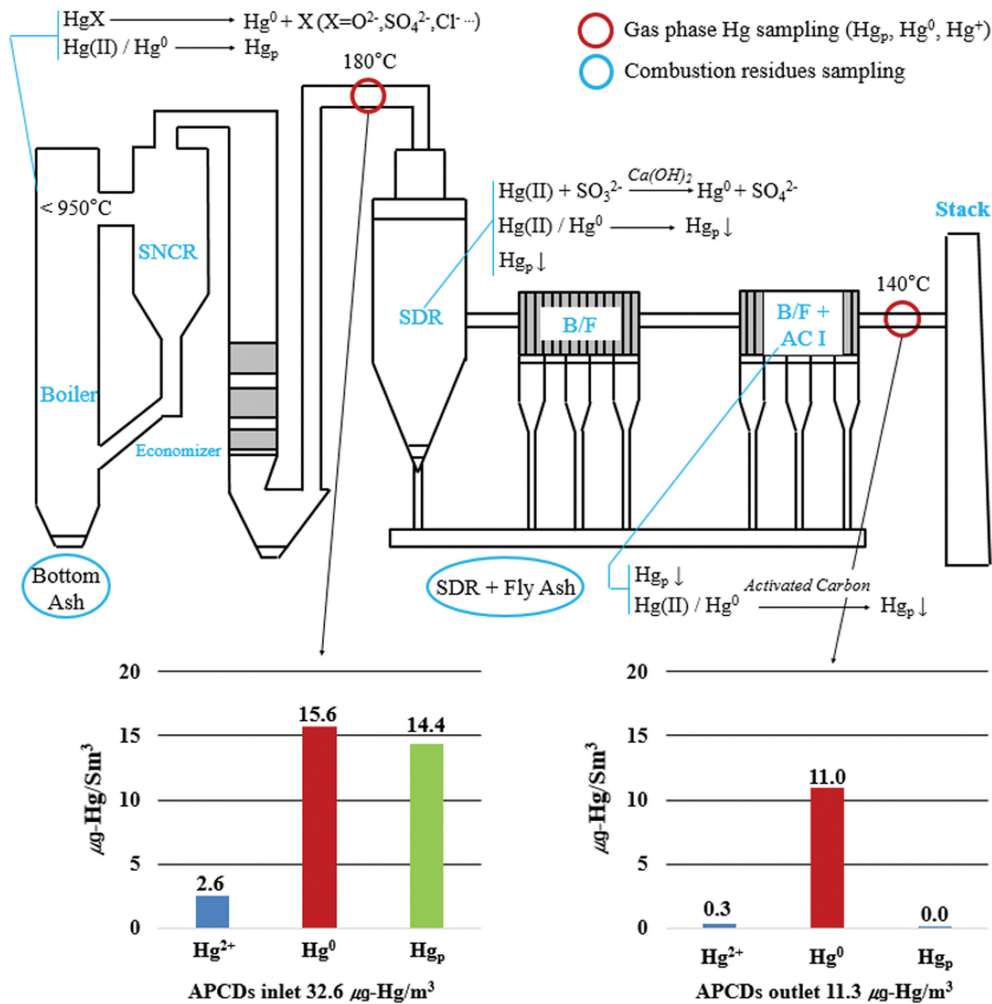


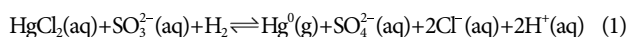
Fig. 1. Hg speciation and removal across APCDs in SRF cogeneration plants.

Table 4. Supplemental data for Hg concentration and speciation in flue gas

Test no.	APCD upstream (before SDR) (µg-Hg/Sm <sup>3</sup> (%))			APCD downstream (stack) (µg-Hg/Sm <sup>3</sup> (%))			Averaged removal efficiency (%)	Stack gas conditions (based on O <sub>2</sub> 6%)	
	Hg <sub>p</sub>	Hg <sup>2+</sup>	Hg <sup>0</sup>	Hg <sub>p</sub>	Hg <sup>2+</sup>	Hg <sup>0</sup>			
1	19.0(49.9)	2.1(5.6)	16.9(44.5)	0.0(0.1)	0.1(0.3)	10.1(99.6)	75	Temp.	140 °C
2	11.3(5.2)	2.4(1.1)	203.0(93.7)	0.0(0.1)	0.6(5.6)	10.3(95.4)		HCl	12 ppm
3	12.9(42.3)	3.1(10.4)	14.5(47.3)	0.0(0.1)	0.3(2.6)	12.6(97.3)		NOx	28 ppm
								SOx	17 ppm
Ave.	14.4(44.1)	2.6(8.0)	15.6(47.9)	0.0(0.1)	0.3(2.7)	11.0(97.2)	CO	6 ppm	
							O <sub>2</sub>	6 %	

there are differences in the characteristics of the Hg in flue gas. These SRF were produced via the short molding process by rotary kiln over 650 °C. During this process some readily volatile pollutants and Hg compounds were separated, then pre-treated fuels were used. Hg has a high oxidation efficiency when it coexists with pollutants such as HCl, NO, and SO<sub>2</sub>. However, this facility had a low fraction of Hg<sup>2+</sup> and concentration of gaseous phase pollutants on using molded SRF and kaolin mixed with fluidized sand. Onsite testing results showed that Hg<sup>0</sup> and Hg<sub>p</sub>, each accounted for about half and Hg<sup>2+</sup> for a small portion of the upstream gas of APCDs. Although the THg concentration range of upstream gas was measured from 30 to 40 µg-Hg/Sm<sup>3</sup>, more than 200 µg-Hg/Sm<sup>3</sup> of irregularly high concentration Hg gas was sometimes measured. It was assumed to be due to the inflow of some Hg concentrated materials with the SRF. Nevertheless, the Hg concentration of the downstream gas from APCDs remained relatively stable. In previous studies, Hg measurements and emission factor estimations were conducted in MSWI with the same APCDs configuration as this facility [12]. The concentration of Hg in the flue gas in APCDs inlet and stack was measured to be 32.04 and 4.18 µg-Hg/Sm<sup>3</sup>, respectively, and these values do not differ significantly from the Hg emission characteristics of the facility.

The first APCD neutralized acidic gases such as SO<sub>2</sub> and HCl by injection of slaked lime with SDR. In previous studies, Agarwal et al. [26] and Li et al. [27] reported the effects of HCl and NO on oxidation of Hg<sup>0</sup> [26,27]. The oxidation efficiency of Hg<sup>0</sup> increased dramatically at the HCl concentration in the range of 0 to 10 ppm. However, it gradually reduced as HCl concentration was over 20 ppm. Onsite testing results show that the concentration of HCl upstream gas was analyzed to be 12 ppm, which is considered proper for Hg oxidation. Also, SO<sub>2</sub> was effective in Hg oxidation when O<sub>2</sub> was at 4% or HCl greater than 5 ppm in flue gas, and the oxidation efficiency of Hg at approximately 100 ppm of SO<sub>2</sub> was estimated to be 60%. However, in the SDR, Hg<sup>2+</sup> would be re-emitted to the chemical reaction as follows [25].



Since the SO<sub>2</sub> concentration of this gas was not significantly higher than 100 ppm, the dominant gas affecting Hg oxidation among the upstream gases was fed as HCl. Therefore, the concentration of Hg<sup>0</sup> in flue gas was reduced by the oxidation reaction; further, Hg<sup>2+</sup> was emitted into ash via adsorption reaction [2]. At this time, Hg discharged in the form of waste might contain HgCl<sub>2</sub> or HgSO<sub>4</sub>. This contributed to an increase in the Hg concentration of leachate [23]. Hg stability and recycling possibility are discussed in the following section.

The second APCD is the combined FF, where ACI is inserted between two FF layers to remove heavy metal by adsorption. The adsorption of Hg using activated carbons has various parameters, such as surface area, gas composition, and impregnated materials. Among them, temperature is the most dominant as a function [28]. Lab-scale experiments results showed that the adsorption efficiency was over 90% at 150 °C and that the adsorption efficiency gradually decreased with the increase in temperature [29]. From the on-site monitoring of the temperature of the stack, it can be seen that, if the operating conditions of the FF chamber were assumed

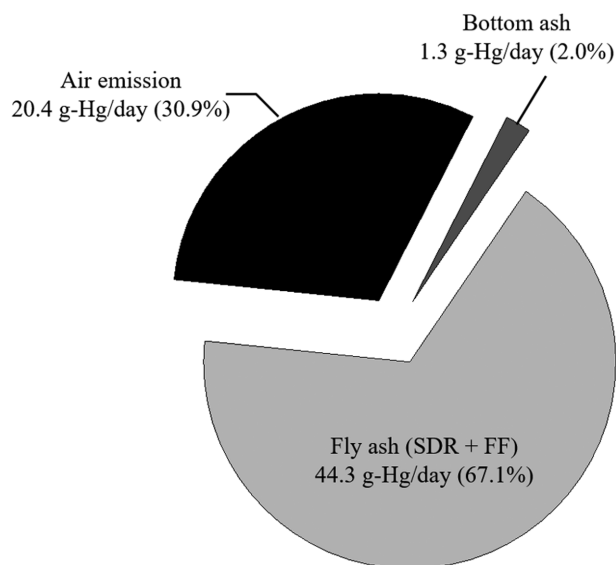


Fig. 2. Mass distribution of Hg from SRF cogeneration plants.

to be under 150 °C, the control performance of Hg by adsorption would have been appropriate. However, the on-site experiment result showed that although Hg<sub>p</sub> and Hg<sup>2+</sup> were nearly eliminated, Hg<sup>0</sup> was still being emitted at approximately 11.0 µg-Hg/Sm<sup>3</sup>.

Mass distribution of Hg was also estimated to identify the major emission media for the management of Hg from SRF utilized for energy generation plants. The fraction of Hg emission from the plant is shown in Fig. 2. The fly ash discharged 18.4 ton/day and Hg content was analyzed as 2.4 (2.3-2.5) mg-Hg/kg. The bottom ash discharged 9.1 ton/day and Hg content was analyzed as 0.15 (0.0-0.2) mg-Hg/kg. Therefore, 44.3 (42.8-46.4) g-Hg/day and 1.36 (0.2-2.1) g-Hg/day of Hg were emitted into fly ash and bottom ash, respectively. The concentration of Hg in the stack emission was 11.0 µg-Hg/Sm<sup>3</sup> and the average volume flow rate was 1,250 Sm<sup>3</sup>/min. Hg emitted into the atmosphere from this plant was estimated at 20.4 (16.3-24.4) g-Hg/day. The waste water was circulated internally after a purification process.

### 3. Hg Emission Factor

In this study, the air emission factor of Hg was estimated along with the Hg mass balance from the SRF power plant. The emission factor for this SRF power plant was 127±25 mg-Hg/ton (5.01±0.98 mg-Hg/GJ). A prior study developed emission factors for various types of industrial facilities [2]. Among them, the average emission factor of 8 MSWIs was estimated at 47.2 (5.9-95.4) mg-Hg/ton. For another study, the average emission factor calculated from 12 circulated fluidized bed type MSWIs was 188±17.7 mg-Hg/ton [19]. In these studies, 8 and 12 MSWI facilities were measured, respectively, and the overall Hg air emission removal efficiency was calculated to be between 75 to 85%. There was no significant difference between the emission factors of the MSWIs, suggesting that the Hg removal efficiency depends on the APCDs configuration more than on the fuel characteristics. The emission factor developed in this study was utilized as data for estimating national air emissions and was included in the technical background report to the global mercury assessment.

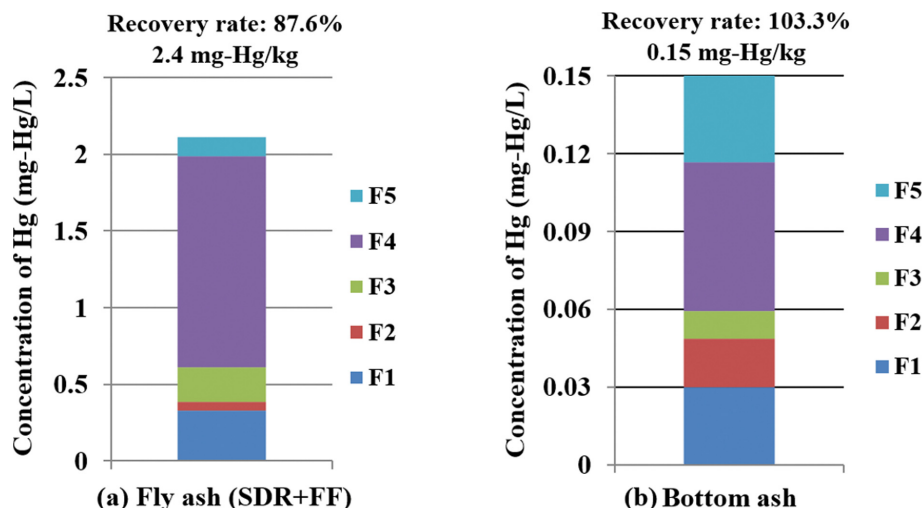


Fig. 3. Results of application of SEP for (a) Fly ash and (b) Bottom ash.

#### 4. Evaluation of Hg Stability in Residues

SEP was applied to understand the characteristics of leaching of Hg in combustion residues (Fig. 3). The leachate recovery ratio during the SEP test of raw fly ash (SDR+FF) and bottom ash accounted for 87.9% and 103.3%, respectively. The typical Hg compounds leached at each step of the SEP are presented in Table 2 [23]. This includes major types of Hg compounds from industrial facilities, such as  $\text{HgCl}_2$ ,  $\text{HgSO}_4$ ,  $\text{HgS}$ ,  $\text{HgO}$ , and  $\text{Hg}^0$ . F1 and F2 have been reported as easily water-soluble Hg compounds and there may be releases via leachate [30]. F4 is known to contain metallic bonds or  $\text{Hg}^0$ , which ensures relative stability to acidity [31]. F1 and F2 of fly ash account for approximately 20% and F4 for 65% of the total leachate content, respectively. F1 and F2 were assumed to have been discharged as waste; F4 was considered to have emitted the  $\text{Hg}^0$  adsorption by the activated carbon injected into the second FF. These experimental results are the supporting data for the behavior and control of the gaseous Hg in the APCDs. Averaged leaching concentration of Hg in bottom ash was  $3 \mu\text{g-Hg/L}$ , not exceeding the standard limit of  $5 \mu\text{g-Hg/L}$ . Therefore, the bottom ash can be classified as general waste.

#### CONCLUSIONS

1. According to the fuel analysis for the Hg assessment of this facility, the input amount of T-Hg for the facility was in the range of 41.6 to 169.6 g/day. The chlorine content in the SRF was in the range of 0.6 to 0.8%.

2. To determine the Hg speciation and removal efficiency of the facility, flue-gas sampling was conducted at the inlet and outlet of APCD. At the inlet of APCD, the particulate and elemental Hg were dominant species in the flue-gas. After passing through APCDs, the elemental Hg was the dominant species because the particulate and oxidized Hg was mostly removed owing to the configuration of APCDs.

3. Based on the Hg SEP results of residues, the fractions of F4 ( $\text{Hg}^0$ ) in the bottom and fly ash were larger than those of the other compounds. In SRF combustion surroundings, mercury that orig-

inated from different wastes was volatilized as elemental mercury at high temperature and then physically adsorbed on porous carbon particles. Finally, during the passage through APCDs, elemental mercury played an important role in the particle growth mechanisms with AC injection and then was bound to the dust cake on FF.

4. For the Hg emission assessment of the facility, the total mass distribution of air emission, bottom ash, and fly ash was observed as 20.4, 1.3, and 44.3 g-Hg/day, respectively. Although elemental mercury was captured by AC injection with FF, it would be desirable for a chemical capturing process to be installed in this SRF plant to avoid emission of mercury into the air. Since the fly ash should be carefully treated as a hazardous waste, the volatile elemental mercury in the fly ash residue should be recovered via thermal desorption before the final landfilling process.

#### ACKNOWLEDGEMENTS

This work has been supported by the Korea Institute of Energy Technology Evaluation and Planning (KETEP) and the Ministry of Trade, Industry and Energy (MOTIE) of the Republic of Korea (No. 20184030202240).

#### REFERENCES

1. United Nations Environment Programme, Minamata convention on Mercury (2019).
2. J. H. Kim, J. M. Park, S. B. Lee, D. Pudasainee and Y. C. Seo, *Atmos. Environ.*, **44**, 2714 (2010).
3. D. Pudasainee, Y. C. Seo, J. H. Sung, H. N. Jang and R. Gupta, *Inter. J. of Coal Geo.*, **170**, 48 (2017).
4. R. Ochoa-G-González, M. Díaz-Somoano and M. Rosa Martínez-Tarazona, *Environ. Sci. Technol.*, **47**, 2974 (2013).
5. United Nations Environment Programme, Global Mercury Assessment (2018).
6. G. Wang, J. Deng, Y. Zhang, Q. Zhang, L. Duan, J. Hao and J. Jiang, *Sci. Total Environ.*, **741**, 140326 (2020).

7. J. H. Sung, S. K. Back, E. S. Lee, H. N. Jang, Y. C. Seo, Y. S. Kang and M. H. Lee, *J. Environ. Sci.*, **80**, 58 (2019).
8. Y. Cao, Z. Gao, J. Zhu, Q. Wang, Y. Huang, C. Chiu, B. Parker, P. Chu and W. P. Pan, *Environ. Sci. Technol.*, **42**, 256 (2008).
9. N. Maamoun, R. Kennedy, X. Jin and J. Urperlainen, *Renew. Sustain. Energy Rev.*, **126**, 109833 (2020).
10. T. Ahmad, J. M. Park, S. G. Keel, J. H. Yun, U. D. Lee, Y. W. Kim and S. S. Lee, *Korean J. Chem. Eng.*, **35**, 9 (2018).
11. Ministry of Environment Korea, Enforcement regulation of the act on the promotion of saving and recycling of resources (2019).
12. K. S. Park, Y. C. Seo, S. J. Lee and J. H. Lee. *Powder Technol.*, **180**, 151 (2008).
13. M. B. Chang, H. T. Wu and C. K. Huang, *Sci. Total Environ.*, **246**, 165 (2000).
14. I. Naruse, R. Yoshiie, T. Kameshima and T. Takuwa, *J. Mater. Cycles. Waste. Manag.*, **12**, 154 (201).
15. J. Wilcox, J. Robles, D. C. J. Marsden and P. Blowers, *Environ. Sci. Technol.*, **37**, 4199 (2003).
16. B. Krishnakumar, S. Niksa, L. Sloss, W. Jozewicz and G. Futsaeter, *Energy Fuels*, **26**, 4624 (2012).
17. T. Ahmad, J. Park, S. Keel, J. Yun, U. Lee, Y. Kim and S. S. Lee, *Korean Chem. Eng. Res.*, **35**, 1823 (2018).
18. S. Yi and Y. C. Jang, *J. Mater. Cycles. Waste. Manag.*, **20**, 19 (2018).
19. L. Chen, M. Liu, R. Fan, S. Ma, Z. Xau, M. Ren and Q. He, *Sci. Total Environ.*, **447**, 396 (2013).
20. ASTM International, ASTM D6784-16 Annual book of ASTM standards, 11.07 (2008).
21. US Environmental Protection Agency, Method 7471A, Mercury in solid or semisolid waste, manual cold vapour technique (1994).
22. US Environmental Protection Agency, Method 7470A, Mercury in liquid waste, manual cold vapor technique (1994).
23. N. S. Bloom, E. Preus, J. Katon and M. Hiltner, *Anal. Chim.*, **479**, 233 (2003).
24. C. P. Kelkar, M. Xu and R. J. Madon, *Ind. Eng. Chem. Res.*, **42** (2003).
25. D. Chen, X. Liu, C. Wang, Y. Xu, W. Sun, J. Cui, Y. Zhang and M. Xu, *Energy Fuels*, **31**, 6455 (2017).
26. H. Agarwal, H. G. Stenger, S. Wu and Z. Fan, *Energy Fuels*, **20**, 1068 (2006).
27. H. Li, C. Y. Wu, Y. Li, L. Li, Y. Zhao and J. Zhang, *Chem. Eng. J.*, **219**, 319 (2013).
28. Z. Mei, Z. Shen, Q. Zhao, W. Wang and Y. Zhang, *J. Hazard. Mater.*, **152**, 721 (2008).
29. S. Yang, D. Wang, H. Liu, C. Liu, X. Xie, Z. Xu and Z. Liu, *Chem. Eng. J.*, **358**, 1235 (2019).
30. S. K. Back, B. M. Jung, E. S. Lee and J. H. Sung, *J. Hazard. Mater.*, **382**, 121094 (2020).
31. E. S. Lee, S. J. Cho, S. K. Back, Y. C. Seo, S. H. Kim and J. I. Ko, *Environ. Pollut.*, **264**, 114761 (2020).